DØnote 4577-Conf, Final

# Search for Heavy $Z'$ Bosons in the Dimuon Channel with 250 pb$^{-1}$ of Data with the DØ Detector


The DØ Collaboration
*URL: http://www-d0.fnal.gov*



(Dated: August 12th, 2004)



We report preliminary results on a search for a heavy partner of the $Z$ boson with Standard-Model-like couplings to fermions in the dimuon channel using $250 \pm 16$ pb$^{-1}$ of data collected in Run II of the Fermilab Tevatron. We set a lower limit on the mass of the $Z'$ boson with the SM-like couplings to fermions of 680 GeV at the 95% confidence level (CL).


*Preliminary Results for Summer 2004 Conferences*

## I. $Z'$ MODELS

A heavy partner of the $Z$ boson, a so-called $Z'$ boson, is found in multiple extensions of the Standard Model (SM). It is particularly popular in extended technicolor models, grand unified theories, models with extra dimensions, and little Higgs models. Depending on the model, couplings of the $Z'$ boson to light fermions could be either SM-like or modified. In some models, $Z'$ couples only to the third generation fermions. A good review of the various extended gauge theory models and references can be found in Ref. [1].

One of the simplest extensions is the *Left-Right Symmetric Model (LRM)* where a right-handed gauge group is added to the electroweak sector restoring parity at high-energy and giving $SU(2)_R \times SU(2)_L \times U(1)$ [2]. The LRM also falls out naturally as a subgroup of $SO(10)$ and an alternative LRM from $E_6$ models, both favored in grand unified theories [3]. Superstring theories also give rise to $E_6$ as the simplest unifying group with a slightly modified $U(1)$ generator for the $Z'$.

This analysis considers a $Z'$ resonance with SM-like coupling to all generations of matter. Although there is no theoretical model for such a $Z'$ boson as it is non-gauge invariant, this reference model is very useful for experimental comparisons [1]. The width of such a $Z'$ boson is proportional to the $Z'$ mass, once all the decay channels are open. The best published direct lower limit on such a $Z'$ boson comes from the CDF experiment in the Tevatron Run I [4], and is 690 GeV at the 95% confidence level (CL). The published DØ Run I limit [5] is 670 GeV. For the current Run II DØ dielectron $Z'$ results see Ref. [6].

The results of this search can be easily reinterpreted as a search for *any* heavy narrow resonance decaying into muon pairs. Examples of such resonances include technirho and techniomega particles found in technicolor models, Randall-Sundrum gravitons, etc.

## II. SEARCH FOR SM-LIKE $Z'$ BOSONS IN THE DIMUON CHANNEL

### A. Monte Carlo Generator

We model the SM background and the effects of $Z'$ via the parton-level LO Monte Carlo (MC) generator of Ref. [7], augmented with a parametric simulation of the DØ detector. The simulation takes into account the acceptance, efficiencies, and resolution of the detector, initial state radiation, and the effect of different parton distributions. We used leading order CTEQ5L [8] parton distributions to estimate the nominal prediction. The parameters of the detector model are tuned using $Z(ee)$ and $Z(\mu\mu)$ data as well as full MC simulation.

The MC includes SM contributions $(Z/\gamma^*)$ and and allows us to model different mass $Z'$ signals in dilepton production. Since the parton-level generator involves only the $2 \rightarrow 2$ hard-scattering process, we model next-to-leading order (NLO) effects by adding a transverse momentum to the dimuon system, based on the measured transverse momentum spectrum of $Z(ee)$ events. We also account for NLO effects in the SM background and $Z'$ signal by scaling the cross sections by a constant $K$-factor of 1.3 [11].

This analysis assumes that detector resolutions dominate the measured width of the $Z'$ resonance. We assume that the internal width of the $Z'$ varies with mass in the following way (as is expected from theory),

$$\Gamma_{Z'} = (\frac{m_{Z'}}{m_Z})\Gamma_Z. \tag{1}$$

Using the standard values for the $Z$ boson ($\Gamma_Z = 2.49$ GeV, $m_Z = 91.19$ GeV) and a $Z'$ mass of 600 GeV, yields an internal width for the $Z'$ of 16 GeV. Variations to the internal width are very small relative to detector resolutions, which are on the order of 200 GeV for a $Z'$ with invariant mass of 600 GeV. Therefore, any changes of the $Z'$ internal width as a function of mass are ignored for this analysis.

### B. Data Selection

The data used for this analysis were recorded between 2002 and 2004, in the Run II of the Fermilab Tevatron. All the data have been reconstructed with the most modern version of the DØ reconstruction program. This data corresponds to a total integrated luminosity of $\approx 250$ pb$^{-1}$ and was collected via a suite of single muon and dimuon triggers, which run unprescaled at all instantaneous luminosities. Given that the analysis is concerned only with high-$p_T$ muons, the trigger is $99 \pm 1\%$ efficient for the signal.

We require at least two muons in the event, with $p_T$ above 15 GeV, which pass data and track quality cuts, have high invariant mass and pass cosmic ray vetoes and isolation selections. Furthermore, due to the fact that our dominate background stems from Drell-Yan events where one of the muons is badly measured, yielding a very high artificial momentum, we apply a fix which corrects this badly measured muon. This fix sets both of the muon's transverse momenta equal to a weighted average based on both muons original $p_T$ measurements and errors. In the case of a Drell-Yan event which has one badly measured (very high $p_T$) muon its transverse momentum is set to a value near the original $p_T$ of the other muon in the event. This is because the error for such a high $p_T$ track is very large and therefore does not contribute much in the calculation of the weighted average. For an event where both muons transverse momenta and errors are similar the new $p_T$ value they are set to will not be very different from the original values.

After the $p_T$ rescaling, we recompute the four-momenta and re-apply the invariant mass selection to form our final data set. This procedure is also applied to the fast MC which generates our background and signal.

This selection leaves us with a sample of 16,796 events, as documented in Table I.

| Selection | Number of events passing cut |
|---|---|
| Starting sample | 115,009 |
| Bad run removal | 108,574 |
| Duplicate events removed | 105,863 |
| Track quality cuts | 65,163 |
| Dimuon invariant mass > 50 GeV | 40,744 |
| Cosmic veto | 25,811 |
| Isolation requirements | 17,193 |
| After $p_T$ fixed re-apply mass cut | 16,796 |

TABLE I: Event selection.

### C. Backgrounds

The SM backgrounds from Drell-Yan and $Z$ boson production are already included in the output of the fast Monte Carlo used to simulate signal. We determine the normalization for this background by fitting the low-mass region of the dimuon mass spectrum to the sum of the Drell-Yan background, with the integrated luminosity being the free parameter of the fit. Since the effects of $Z'$ are negligible at low invariant dimuon masses, this technique is not biased by a possible presence of the signal in our data.

The cuts made to remove cosmic ray events are chosen such that the level of dimuon events originating from this process are negligible. Similarly the isolation criteria used in this analysis eliminates all but a negligible level of dimuon events that originate from $b\bar{b}$ production.

All other physics backgrounds that result in a dimuon final state are negligible.

### D. Comparison between the Data and Background

The comparison between the data sample of 16,796 events and predicted background is illustrated in Figure 1.

Because this analysis is concerned with very high mass events and to help quantify the agreement between the data and the background in the mass spectrum, we calculate the prediction for the background above certain mass cutoff and compare it with the data for a number of mass cutoffs. The results are summarized in Table II.

### E. Systematics

We consider various sources of systematic uncertainties for signal and background. The uncertainty on the background is dominated by the uncertainty on the shape of the NLO corrections (i.e., energy dependence of the $K$-factor, 10%), choice of parton distribution functions (5%), possible residual $p_T$ dependence on the efficiency (5%), choice of $p_T$ smearing in the fast MC (4%), and the fast MC to data normalization (1%). The normalization used in this analysis is referred to as the effective luminosity and is the factor that scales the NLO $Z$-peak cross section to the data in the mass region less than 120 GeV. By using the effective luminosity we reduce the systematic error on the MC to data normalization, which otherwise would be larger if the errors from the luminosity, efficiencies and so on, were calculated independently and added in quadrature. While this helps with the systematic error on the background, we still utilize the luminosity value and error found from the DØ luminosity system of $250 \pm 16$ pb$^{-1}$ for the input

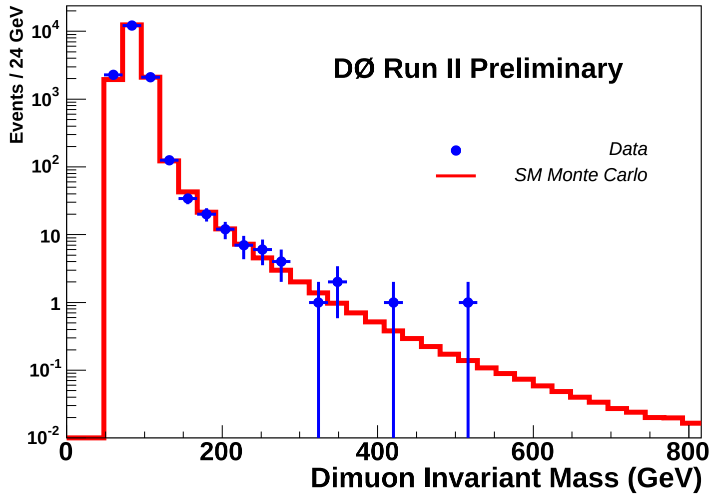


FIG. 1: Dimuon invariant mass distributions for data (points) and background (histogram).

| Minimum $M_{\mu\mu}$ | Expected background | Number of candidates |
|---|---|---|
| 120 GeV | 221.0 | 213 |
| 150 GeV | 84.9 | 73 |
| 180 GeV | 43.6 | 43 |
| 210 GeV | 24.8 | 24 |
| 240 GeV | 15.1 | 15 |
| 270 GeV | 9.6 | 9 |
| 300 GeV | 6.4 | 5 |
| 330 GeV | 4.4 | 5 |
| 360 GeV | 3.2 | 2 |
| 390 GeV | 2.3 | 2 |
| 420 GeV | 1.7 | 1 |
| 450 GeV | 1.3 | 1 |
| 480 GeV | 1.0 | 1 |
| 510 GeV | 0.83 | 1 |
| 540 GeV | 0.67 | 0 |

TABLE II: Comparison between the data and expected background for events above certain dimuon mass cutoffs. The middle column shows the number of predicted background events. While the last column shows the number of candidate events seen.

into the limit setting code and procedure. This is done for purely practical reasons and will tend to overestimate the errors in the limit setting procedure and is therefore conservative.

The signal acceptance is found by dividing the generator level output by output which contains the acceptance information from the fast MC versus invariant mass. This acceptance versus invariant mass distribution is then fit using a polynomial which is evaluated at the mean of the fitted signal resonance.

Errors on the acceptance are determined by varying the momentum smearing parameters in the fast MC by $\pm 1\sigma$ and reevaluating the acceptance calculation. Variations seen were on the 0.5% level, therefore to be conservative we use and error of 1% for all the signal acceptances in this analysis. Table III and Table IV summarize the systematic uncertainties used in this study.

| Source of systematics | Uncertainty |
|---|---|
| $K$-factor | 10% |
| Choice of p.d.f. | 5% |
| $p_T$ dependence on efficiency | 5% |
| Choice of fast MC $p_T$ smearing | 4% |
| Fast MC to data normalization | 1% |
| Total | 13% |

TABLE III: Sources of systematic uncertainty on the background calculated cross section.

| | Value | Error |
|---|---|---|
| Luminosity | $250\text{pb}^{-1}$ | 6.5% |
| Acceptance | 0.470-0.555 | 1.0% |
| Background | See Table III | 13% |
| Total | | 15% |

TABLE IV: Summary of the limit setting inputs and errors.

### F. Optimum Window

This procedure follows closely the ideas previously established in a similar analysis [12] to enhance the Gaussian significance, i.e. $S/\sqrt{B}$ for such a search. The procedure uses fits to the different $Z'$ signals generated with the fast MC to determine the width of the reconstructed resonances. In a similar fashion the falling Drell-Yan background spectrum from the fast MC simulation is fit to allow the determination of the amount of background with different mass windows. This analysis uses an asymmetric window, that is to say that we determine only the lower mass cut location with this procedure and count events out to infinite masses (which we approximate with a cut of 1500 GeV).

The results of the counting experiments for different $Z'$ masses and each mass window are summarized in Table V.

| $Z'$ Mass | 200 GeV | 300 GeV | 400 GeV |
|---|---|---|---|
| Acceptance | 0.459±0.005 | 0.499±0.005 | 0.521±0.005 |
| Cut Window | 151-1500 GeV | 202-1500 GeV | 226-1500 GeV |
| Background | 91.4±11.9 | 30.71±4.0 | 20.2±2.6 |
| Data | 76 | 29 | 19 |
| $Z'$ Mass | 500 GeV | 600 GeV | 700 GeV |
| Acceptance | 0.534±0.005 | 0.542±0.005 | 0.546±0.006 |
| Cut Window | 230-1500 GeV | 232-1500 GeV | 240-1500 GeV |
| Background | 18.3±2.4 | 18.3±2.4 | 15.8±2.1 |
| Data | 18 | 18 | 16 |

TABLE V: Summary of acceptance, data, and background.

Since the data in each window are consistent with the expected background, we proceed with setting limits on the existence of the $Z'$ resonance.

### G. Limits on the $Z'$ cross section

Assuming that the acceptance for *any narrow resonance* is similar to that of the $Z'$ the results shown here can give a conservative estimate for any such resonance decaying into dimuons, e.g. technirho or techniomega. Our limits can then be reinterpreted in a straightforward manner for a variety of models without knowing the details of the DØ apparatus or the analysis.

A standard Bayesian limit-setting procedure with the signal and background systematics discussed above is applied. This analysis finds 95% CL experimental limits on $\sigma \times BR(Z' \rightarrow \mu\mu)$ which are summarized in Table VI and in Figure 2. The theoretical cross sections used are scaled by the same $K$-factor of 1.3 used for the background. Figure 2 also shows the theoretical $\sigma \times BR(Z' \rightarrow \mu\mu)$ versus invariant mass. The lines to ether side of the theoretical curve are $\pm 1\sigma$ errors on the signal cross section which are not included in the limit setting procedure. This error on the signal cross section is assumed to be $\pm 11\%$ and is determined from a 10% error for the $K$-factor and 5% error from the choice of parton distribution functions. The nominal theoretical curve crosses the experimental limit at 682 GeV, which defines the experimental lower mass limit on a SM-like $Z'$ decaying into two muons and is indicated in Figure 2 with a arrow. The limit would be 670 GeV if we were to use the lower theoretical band and 694 GeV if the high theory band was used, this is shown in Figure 2 by dashed vertical lines.

## III. CONCLUSIONS

We performed a search for heavy $Z'$ resonances decaying into the dimuon channel using $250 \pm 16$ pb$^{-1}$ of data collected by the DØ Experiment at the Fermilab Tevatron in 2002-2004 (Run II). The data are in excellent agreement with Drell-Yan production and do not exhibit any evidence for new physics beyond the Standard Model, so we use

| $Z'$ Mass (GeV) | $\sigma \times BR(Z' \to \mu\mu)$ (pb) theoretical (LO×1.3) | $\sigma \times BR(Z' \to \mu\mu)$ (pb) 95% CL Experimental Limit |
|---|---|---|
| 200 | 18.76 | 0.191 |
| 300 | 4.475 | 0.110 |
| 400 | 1.379 | 0.084 |
| 500 | 0.472 | 0.083 |
| 600 | 0.176 | 0.082 |
| 700 | 0.067 | 0.079 |

TABLE VI: Theoretical and measured $\sigma \times BR(Z' \to \mu\mu)$

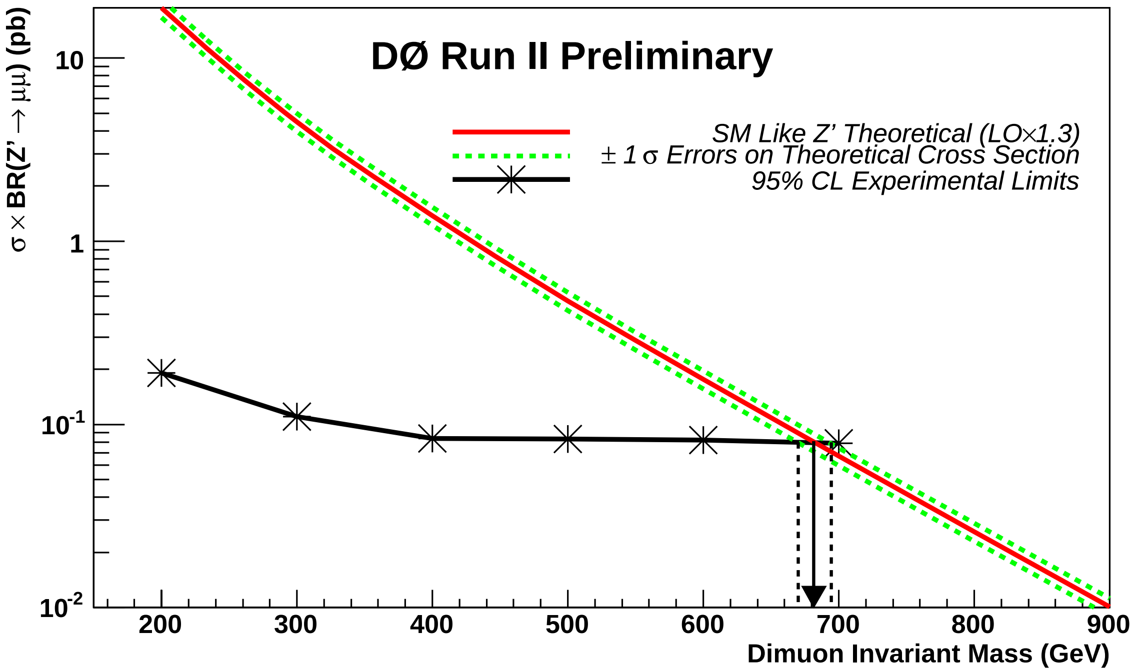


FIG. 2: The 95% CL limits on $\sigma \times BR(Z' \to \mu\mu)$. The arrow indicates the mass limit attained in this analysis of 680 GeV for a SM-like $Z'$. Dashed vertical lines indicate mass limits that would be found if the theoretical cross section was varied by $\pm 1\sigma$.

them to set limits on the existence of the $Z'$ boson. A lower limit on its mass has been set at 680 GeV at the 95% CL, assuming SM-like couplings to fermions.

### Acknowledgments

We thank the staffs at Fermilab and collaborating institutions, and acknowledge support from the Department of Energy and National Science Foundation (USA), Commissariat à L'Energie Atomique and CNRS/Institut National de Physique Nucléaire et de Physique des Particules (France), Ministry for Science and Technology and Ministry for Atomic Energy (Russia), CAPES, CNPq and FAPERJ (Brazil), Departments of Atomic Energy and Science and Education (India), Colciencias (Colombia), CONACyT (Mexico), Ministry of Education and KOSEF (Korea), CONICET and UBACyT (Argentina), The Foundation for Fundamental Research on Matter (The Netherlands), PPARC (United Kingdom), Ministry of Education (Czech Republic), A.P. Sloan Foundation, Civilian Research and Development Foundation, Research Corporation, Texas Advanced Research Program, and the Alexander von Humboldt Foundation.

[1] M. Cvetic and S. Godfrey, hep-ph/9504216, 1995.

[2] J.C. Pati and A. Salam, *Phys. Rev. Lett.* **31**, 661 (1973); R.N. Mohapatra, *Phys. Rev.* **D11**, 2558 (1975); G. Sejanovic and R.N. Mohapatra, *Phys. Rev.* **D12**, 1502 (1975).

[3] J.L. Hewett and T.G. Rizzo, *Phys. Rep.* **183**, 193 (1989).; R.N. Mohapatra, *Unification and Supersymmetry*, Springer, 1992.; E. Ma, *Phys. Rev.* **D36**, 274 (1987).; K.S. Babu *et al*, *Phys. Rev.* **D36**, 878 (1987).

[4] CDF Collaboration, F. Abe *et al.*, Phys. Rev. Lett. **79**, 2192 (1997).

[5] DØ Collaboration, V.M. Abazov *et al.*, Phys. Rev. Lett. **87**, 061802 (2001).

[6] DØ Collaboration, DØ Note 4375-Conf (2004), `http://www-d0.fnal.gov/Run2Physics/WWW/results/NP/N03/N03.pdf.`

[7] K. Cheung and G. Landsberg, Phys. Rev. D **62**, 076003 (2000).

[8] H.L. Lai *et al.*, Phys. Rev. **D51**, 4763 (1995).

[9] F. Del Aguila, M. Quiros and F. Zwirner, Nucl Phys. **B287**, 419 (1987).

[10] D. London and J.L. Rosner, Phys. Rev. **D34**, 5, 1530 (1986).

[11] R. Hamberg, W.L. Van Neerven, and T. Matsura, Nucl. Phys. B**359**, 343 (1991).

[12] G. Landsberg and K.T. Matchev, Phys. Rev. D **62**, 035004 (2000).

[13] T. Sjostrand, P. Eden, C. Friberg, L. Lonnblad, G. Miu, S. Mrenna, and E. Norrbin, Comp. Phys. Comm. **135**, 238 (2001).